Reprinted from Preprint Volume: 17th Conference on Radar Meteorology, Oct. 26-29, 1976; Seattle Wash.; Published by American Meteorological Soc., Boston, Ma.

ANALYSIS OF GATE RADAR DATA FOR A TROPICAL CLOUD CLUSTER IN AN EASTERLY WAVE

Colleen A. Leary and Robert A. Houze, Jr.

Department of Atmospheric Sciences
University of Washington
Seattle, Washington

1. INTRODUCTION

One objective of the GARP[1] Atlantic Tropical Experiment (GATE) radar program was to investigate the internal structure of tropical cloud clusters. The high time and space resolution of quantitative radar observations obtained over large horizontal areas during GATE (Austin, 1975; Hudlow, 1975a) makes possible detailed studies of individual cloud systems.

This paper describes the three-dimensional structure and life history of a cloud cluster which remained within range of the C-band (5.30 cm wavelength) radar on board the U.S. NOAA ship Oceanographer (see front cover) from 0000 to 2300 GMT on 5 September 1974.

A complete sequence of PPI scans for twelve tilt angles from 0.6° to 22° was recorded every 15 min both digitally and photographically, and a PPI scan at the base tilt angle (0.6°) was recorded photographically at the intermediate 5 min intervals. More complete descriptions of the radar data are given by Hudlow (1975a and b).

[1]Global Atmospheric Research Program

2. LARGER SCALES OF MOTION

Fig. 1 shows the visible cloud pattern observed by satellite at 1200 GMT on 5 September. The cloud cluster centered at 9.5°N 21°W, with its southwestern portion within range of the Oceanographer radar, is the feature described in this paper. This cluster had a lifetime of about a day, forming near 18°W at 0000 GMT on 5 September, moving westward and dissipating near 24°W at about 0000 GMT on 6 September.

The cloud cluster was a transient feature located in the trough of a synoptic-scale easterly wave, which had a lifetime of at least a week. The trough, best defined in the 700-mb wind field, originated over the African continent on 3 September, and was still an identifiable feature in the 700-mb flow on 10 September, when it crossed 40°W. Over this time period the trough moved at an average speed of 6 m s^{-1}. Its wavelength was about 2000 km. Not only was the wave in the easterly flow larger in horizontal scale and longer-lived by about an order of magnitude than the cloud cluster, but it was associated with at least one other cloud cluster, that located at 9°N 25°W in Fig. 1.

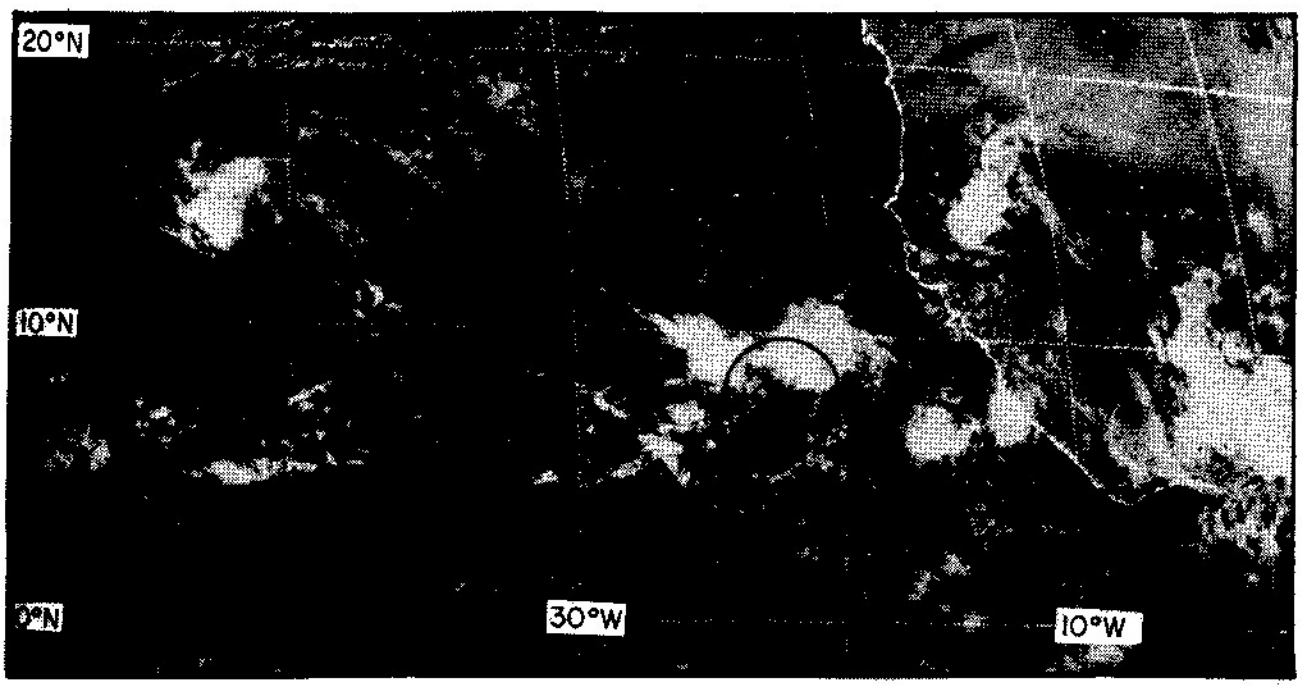

Fig. 1. SMS-1 satellite photograph of the visible cloud pattern over the GATE area at 1200 GMT on 5 September 1974. The circle outlines the range of the Oceanographer radar.

3. EVOLUTION OF THE LOW-LEVEL RADAR ECHO PATTERN

The precipitation located under the cirrus shield of the cloud cluster seen in Fig. 1 comprised a cohesive group of component radar echoes which formed a recognizable physical entity from its first appearance at the northeastern edge of the radarscope at 0000 GMT on 5 September until its demise close to the Oceanographer at about 0000 GMT on 6 September. The growth and decay of this echo group was consistent with the life cycle of the cloud cluster shown by satellite imagery.

During its life cycle the radar echo pattern of the mesoscale precipitation system evolved from a narrow band to an extensive, rather amorphous area of precipitation. We divided this process into five stages, based upon a detailed examination of all the PPI photographs of the radarscope at the lowest tilt angle for 5 September. PPI's selected to illustrate the system's evolution are shown in Fig. 2.

a. 0000 to 0600 GMT

During this first phase, the mesoscale radar pattern appeared as a band (indicated by arrows in Figs. 2a and b). Isolated echoes developed between the ship and the band, but the band remained easy to distinguish from other echoes on the scope. The band moved southwestward at 3 m s^{-1} with the most intense echoes close to the leading edge of the band.

b. 0600 to 1000 GMT

In its second phase of development the mesoscale echo pattern changed markedly when an extensive area of light precipitation developed to the rear of the leading line of intense echoes (Fig. 2c). Other echoes on the radarscope (mainly to the northwest of the ship) grew and intensified during this period. The mesoscale system continued to propagate southwestward at 3 m s^{-1}.

c. 1000 to 1200 GMT

In this relatively short transition stage, the light-rain area to the rear of the band of most intense echoes first shrank, then was re-established. The most intense echoes still occurred at the leading edge, which had acquired a curved character, with the Oceanographer lying close to the radius of curvature (Fig. 2d). Part of this curvature was due to the incorporation of echoes from the northwest quadrant into the mesoscale system.

d. 1200 to 1500 GMT

During this phase the area covered by the radar echo reached its maximum extent (Fig. 2e), incorporating most of the echoes on the radarscope. The leading edge still contained the most intense echoes, but had lost its line-like appearance. The area of lighter rain behind the leading edge had expanded greatly, including what formerly had been intense echo cores. The entire southeastern portion of the echo pattern weakened and dissipated during the interval.

e. 1500 to 2300 GMT

During this period, represented by Fig. 2f, the system was decaying. The leading edge of the system became ill-defined and ceased to propagate. The echo pattern was obscured somewhat by attenuation (possibly due to rain on the radome) when rain began to fall at the ship.

4. THREE-DIMENSIONAL FEATURES OF THE RADAR ECHO PATTERN

In order to investigate the three-dimensional structure of the radar echo pattern, we constructed RHI's from the digital data recorded on magnetic tape. Using the calibration equations of Hudlow (1975b), we processed the digital data tapes for 5 September by unpacking the data, converting the signal intensities to units of dbz, and plotting these in RHI format. Our computer program preserved accuracy without degrading the data by plotting a special symbol at locations where the returned signal, although above the noise level, was so low as to fall at the unreliable end of the calibration curve. Retaining these low signal values proved essential in delineating the three-dimensional structure of the mesoscale system.

Three of the thousands of RHI's plotted for 5 September are shown in Fig. 3 to illustrate characteristic features of the echo pattern. At 1045 GMT (Figs. 3a and 2d) the RHI through azimuth 29° intercepted an intense portion of the echo line. The vertical character of the intensity contours clearly establishes the convective nature of the precipitation. The most intense precipitation fell directly beneath the tallest echo.

An overhang of light precipitation extends 38 km ahead of precipitation at the surface in Fig. 3a. Its position ahead of the surface precipitation pattern is consistent with the 200-mb wind velocity of 18 m s^{-1} from the northeast (azimuth 055°) observed at the Oceanographer at 1200 GMT. This 200-mb wind speed exceeded the speed of propagation of the surface precipitation pattern from nearly the same direction, by a factor of six. The overhang probably delineates the detrainment level for a large portion of the mesoscale system, implying that detrainment took place over a layer several kilometers thick.

At 1300 GMT (Figs. 3b and 2e) the cross section along azimuth 19° shows a broadened echo pattern, with the highest precipitation rate close to the leading edge, and the overhang extending 12 km ahead of rainfall near the surface. To the rear of the most intense convective precipitation, at ranges greater than 110 km, light rain fell over another 80 km. The absence of sharp horizontal reflectivity gradients suggests that the precipitation behind the leading edge was more stratiform than convective.

At 1800 GMT (Figs. 3c and 2f) the cross section along azimuth 29° reveals a much-diminished echo pattern. A rudimentary anvil extends slightly ahead of the remains of the leading edge of intense precipitation, now centered at a range of 63 km. At ranges greater than 65 km, the precipitation pattern takes on a less convec-

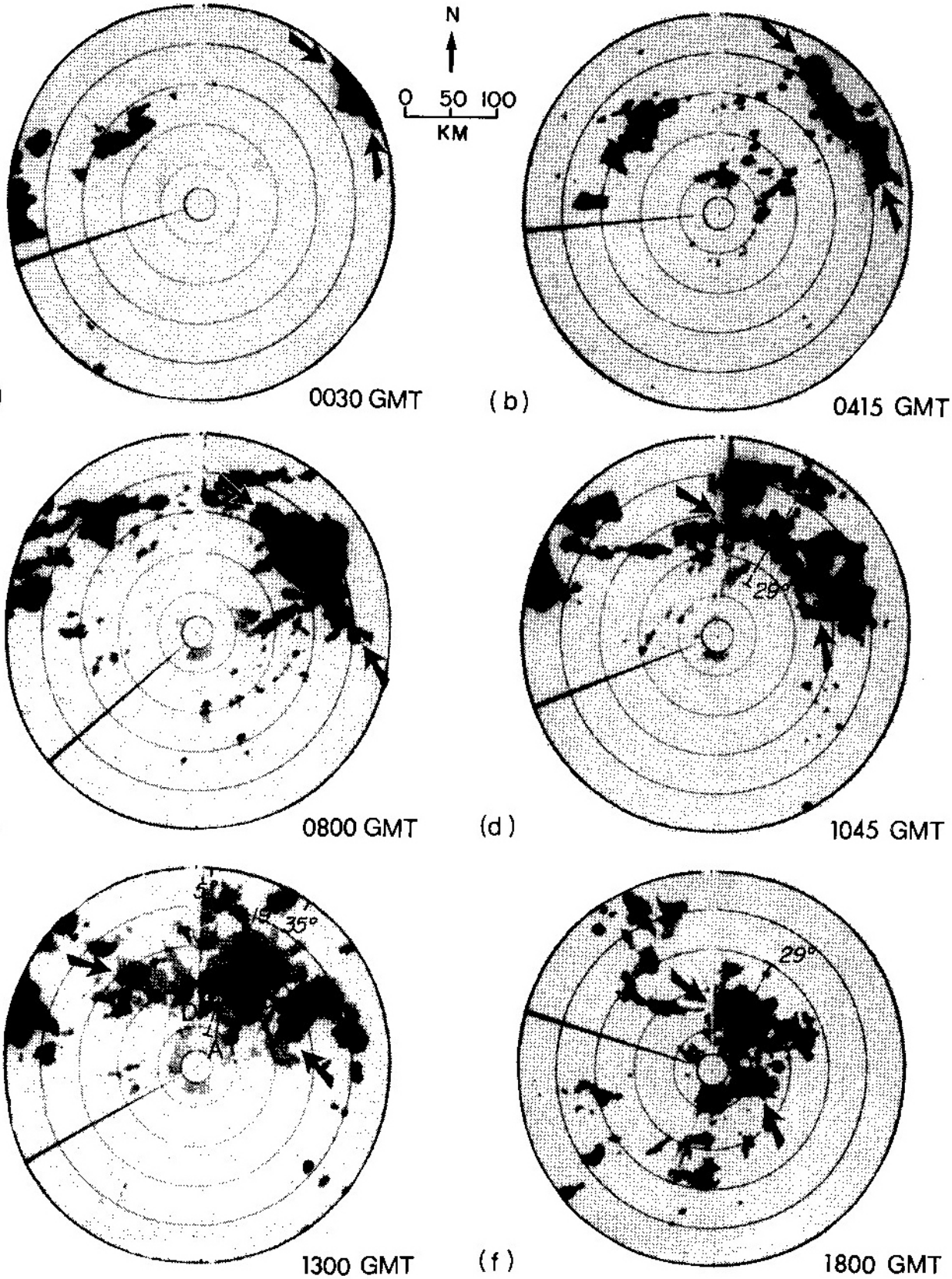

Fig. 2. PPI displays of Oceanographer radar, 5 September 1974. Shading thresholds are for minimum detectable echo (gray), 28 dbz (black), 36 dbz (white), and 44 dbz (gray). Radial line indicates ship heading (a 20° sector was blocked by the ship's superstructure in this direction). Arrows indicate band of most intense echoes. Letters refer to features in text. Dashed lines show locations of RHI's in Figs. 3a-c. Azimuths are labeled in degrees.

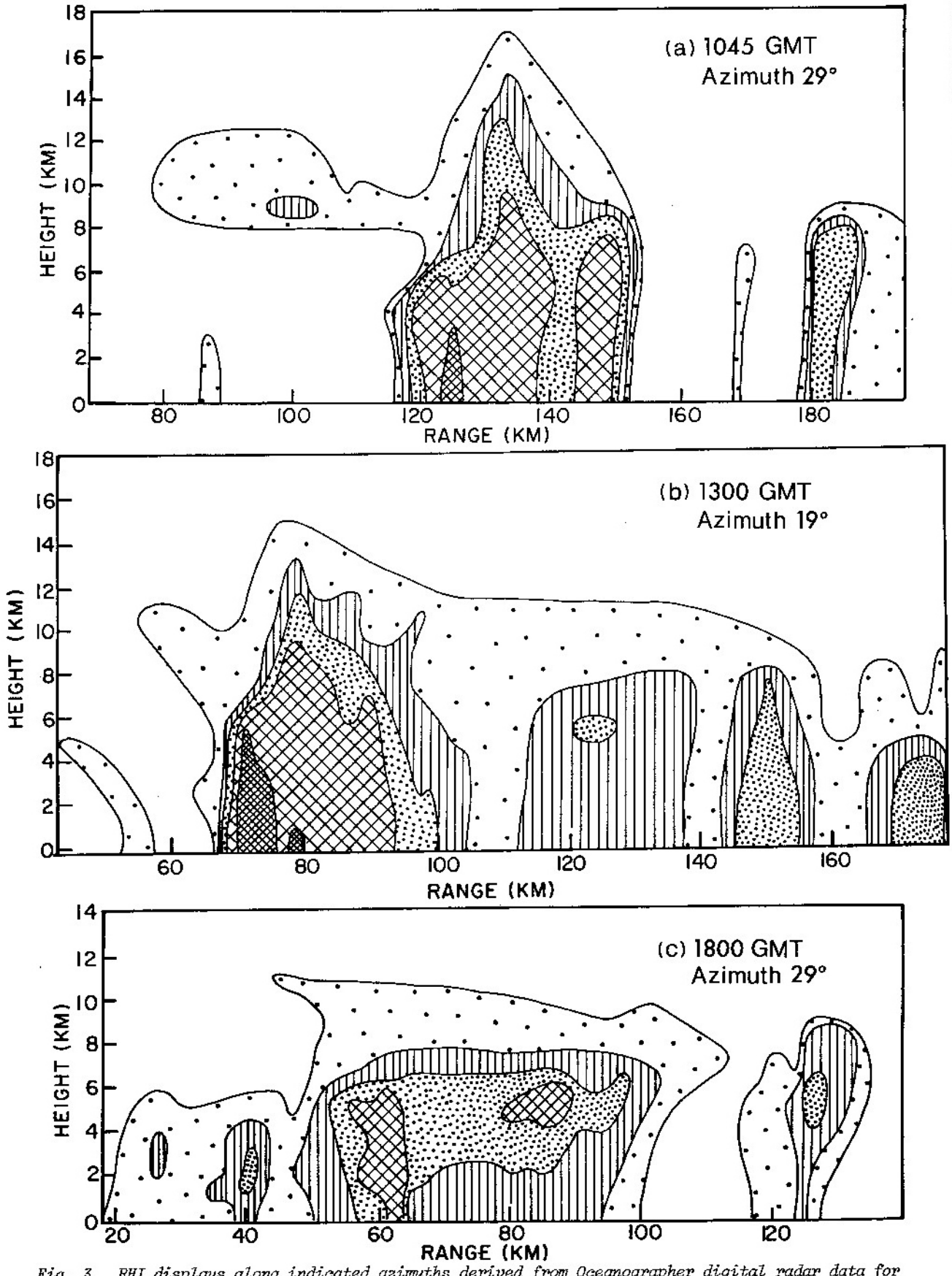

Fig. 3. RHI displays along indicated azimuths derived from Oceanographer digital radar data for 5 September 1974. Inside contours are for 20, 25, 30 and 40 dbz. Outside contour is boundary of weakest detectable echo.

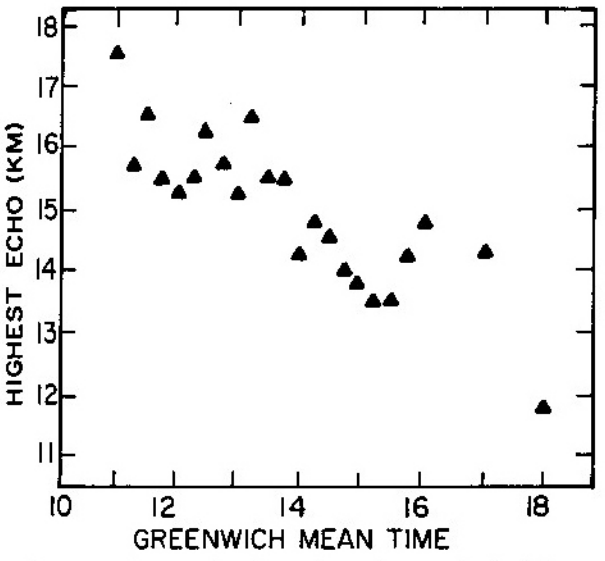

Fig. 4. Time variation of maximum echo height detected by Oceanographer radar on 5 September 1974.

tive and more stratiform character, with suggestions of a melting band in the vicinity of the 0C isotherm at a height of about 4.5 km.

Echo top heights associated with the cloud cluster provide a useful measure of the intensity of this convective system. The highest echo top observed at any azimuth and range, as determined from the RHI's, is plotted in Fig. 4 as a function of time during the period from about 1100 to 1800 GMT. Before 1100 GMT the tallest echoes were located more than 125 km from the radar, and we considered estimates of their heights unreliable because (i) the vertical resolution was poor at these ranges and (ii) small uncertainties in tilt angle

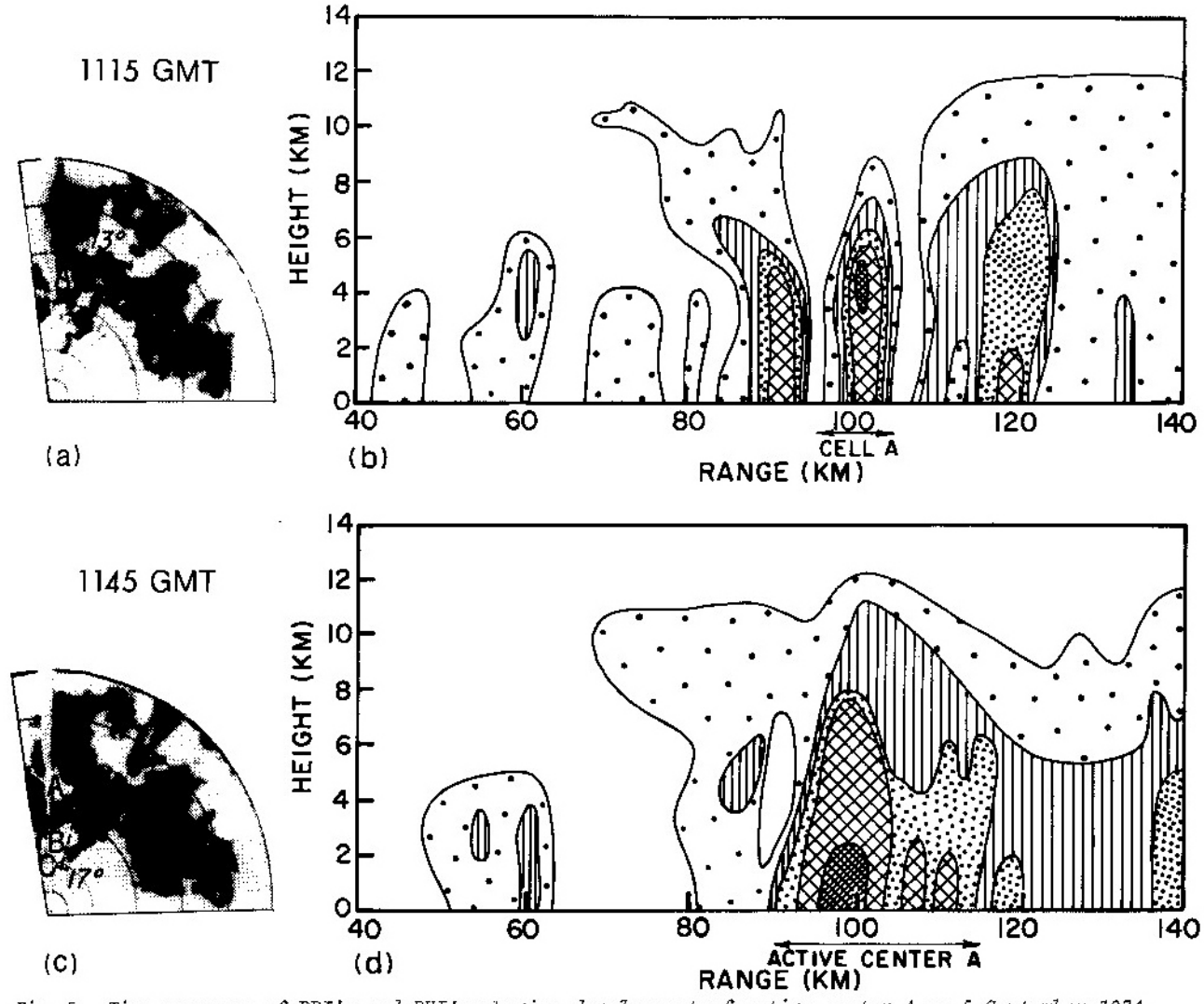

Fig. 5. Time sequence of PPI's and RHI's showing development of active center A on 5 September 1974. Dashed line in PPI indicates azimuth (°) of the corresponding RHI at each time. Letters in PPI's denote features discussed in text. Formats of PPI's and RHI's are explained in captions of Figs. 2 and 3, respectively.

resulted in large uncertainties in height. To a smaller extent these uncertainties are inherent in the information plotted in Fig. 4, which should be interpreted as estimates of maximum echo top height for the mesoscale system accurate to about ±1 km. The gradual decrease in the intensity of the system with time appears clearly as a gradual lowering of the maximum echo height in Fig. 4. This result is consistent with the idea that the deepest convection was the most vigorous. Fig. 4 suggests that if convection in this system ever achieved a steady state, it was for periods of time short compared to the lifetime of the system; for example, from 1115 to 1345 GMT.

5. SMALL-SCALE ORGANIZATION WITHIN THE RADAR ECHO PATTERN

Both the PPI photographs (Fig. 2) and the RHI profiles (Fig. 3) show that the most intense precipitation in the cloud cluster fell in smaller subareas of the larger echo pattern, and that these were separated by regions of lighter precipitation. We refer to the subareas of intense precipitation (which were generally in the 100-1000 km^2, or C-scale, size range) as active centers because they were the fundamental structural entities of the radar echo pattern during its entire lifetime. Active centers had several common features:

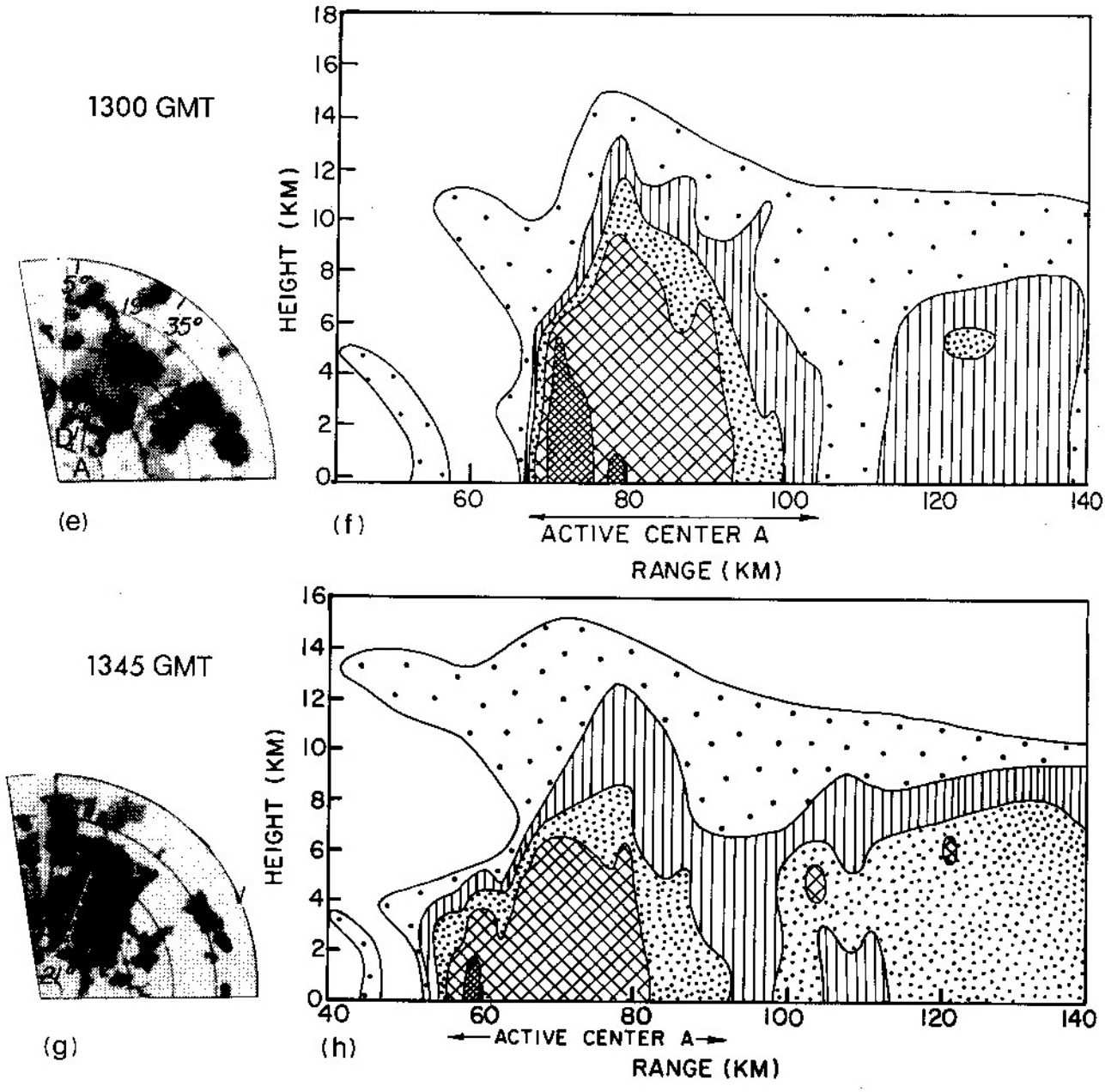

Fig. 5. Continued from previous page.

--They were much smaller than the overall echo pattern, but larger than a single convective cell.

--Active centers contained the most intense convection of the entire echo pattern.

--Active centers contained more than one convective cell. In this respect they resembled the multicell thunderstorms described by Byers and Braham (1949) and the small mesoscale areas (SMSA's) described by Austin and Houze (1972).

--Active centers had lifetimes (typically 1-3 h) which were longer than the lifetime of a convective cell, and short compared to the lifetime of the larger echo pattern.

--Since the highest echoes produced the greatest surface rainfall rates, the most intense period in the lifetime of active centers nearly coincided with the highest cells.

--At any given time, one or more active centers existed within the larger radar echo pattern.

--Active centers, as well as individual cells within them, tended to appear near the southwestern (leading) edge of the main echo pattern, and dissipate by joining the light rain area behind the leading edge. In this respect the active centers resembled the squall line elements described by Houze (1976).

One active center reached its maximum intensity at 1300 GMT (Fig. 2e), occupying azimuths between 5° and 35°. On the RHI section through its most intense portion (Fig. 3b), the active center occupied the range interval between 68 km and 90 km. The life history of this active center (illustrated in Fig. 5) began about 1115 GMT when a small echo intensified just southwest of the main echo pattern (A in Fig. 5a). An RHI profile through an intense portion of this small echo (Fig. 5b) shows that its center, at a range of 100 km, was sandwiched between the main echo pattern at greater range and other less intense echoes closer to the ship. The light precipitation at the 10 km level from range 70 to 90 km may have been due, not to the cell beneath it, but to blowoff from the main echo to the northeast.

Further cellular development subsequently took place on the eastern side of the small echo until at 1145 GMT the site of the formerly small echo (A in Fig. 5 a-b) was occupied by an active center (A in Fig. 5 c-d), which contained the most intense convection within the large-scale echo pattern. The RHI through the most intense portion of active center A at 1145 GMT (Fig. 5d) shows that the upper-level overhang extended 18 km ahead of the intense surface precipitation.

Between 1145 and 1300 more cellular development took place to the south, east, and west of the location of the active center at 1145 GMT. In particular, two echoes (B and C in Fig. 5c) became the site of a distinct southwestward extension of active center A at 1300 GMT (D in Fig. 5e). At 1300 GMT active center A reached its maximum intensity and area covered. The RHI through the most intense portion of active center A (Fig. 5f) shows a particularly sharp horizontal gradient of rainfall rate at the leading edge of the active center, where the rainfall is most intense.

After 1300 GMT active center A declined in intensity as development to the east created a new active center which by 1345 GMT was located at E in Fig. 5g. Even though somewhat less intense, the original active center A retained an impressive vertical structure, as shown by an RHI (Fig. 5h) through the most intense portion at 1345 GMT. The decline of the active center A proceeded rapidly after 1345 GMT.

CONCLUSION

Active centers such as A and E provide a framework within which the combined effects of many individual convective cells can be assessed. The continuity in time and space shown by active centers bridges the gap between the convective scale and larger scales and establishes a descriptive tool for use in studying the internal structure of cloud clusters.

We plan to evaluate the convective transports of mass and heat accomplished within individual active centers as a first step in computing budgets of mass, heat, and moisture for the precipitating area of the cloud cluster as a whole. Convective rain which fell in a particular area during a specified time will be assigned to the appropriate activity center. Our large collection of vertical cross sections will enable us to determine the echo heights corresponding to each center. This information will serve as input to model calculations (similar to those of Austin and Houze, 1973; Houze, 1973; and Houze and Leary, 1976) of convective transports in each active center. The resulting budgets of mass, heat, and moisture will enable us to investigate the roles of individual active centers within the larger-scale cloud cluster, and the combined budgets for all the active centers in the precipitating system will permit an investigation of the interaction of the whole population of precipitating cumulus clouds with its large-scale environment.

ACKNOWLEDGMENTS

Dr. Michael D. Hudlow of the NOAA Center for Experiment Design and Data Analysis provided helpful advice and documentation for handling the Oceanographer radar data tapes. This research was supported by the Global Atmospheric Research Program, National Science Foundation, and the U.S. GATE Project Office, National Oceanic and Atmospheric Administration, Grant OCD-14830.

REFERENCES

Austin, P. M., 1975: GATE - A summary of objectives, the experiment and the role of radar. Preprints 16th Radar Meteorology Conf., Houston, Amer. Meteor. Soc., 182-185.

_____, and R. A. Houze, Jr., 1972: Analysis of the structure of precipitation patterns in New England. J. Appl. Meteor., 11, 926-935.

_____ and _____, 1973: A technique for computing vertical transports by precipitating cumuli. J. Atmos. Sci., 30, 1100-1111.

Byers, H. R. and R. R. Braham, Jr., 1949: The Thunderstorm. Washington, D.C., U.S. Weather Bureau, 287 pp.

Houze, R. A., Jr., 1973: A climatological study of vertical transports by cumulus-scale convection. J. Atmos. Sci., 30, 1112-1123.

_____, 1976: GATE radar observations of a tropical squall line. Preprints 17th Radar Meteorology Conf., Seattle, Amer. Meteor. Soc.

_____, and C. A. Leary, 1976: Comparison of convective mass and heat transports in tropical easterly waves computed by two methods. J. Atmos. Sci., 33, 424-429.

Hudlow, M.D., 1975a: Collection and handling of GATE shipboard radar data. Preprints 16th Radar Meteorology Conf., Houston, Amer. Meteor. Soc., 186-193.

_____, 1975b: Documentation for GATE Oceanographer Radar Film. GATE Processed and Validated Data, Available from World Data Center, National Climatic Center, Asheville, North Carolina, 50 pp.